Nuclear Engineering and Design 239 (2009) 735–748

Contents lists available at ScienceDirect

Nuclear Engineering and Design

journal homepage: www.elsevier.com/locate/nucengdes

Analytical benchmarks for verification of thermal-hydraulic codes based on sub-channel approach

O. Merroun[a,*], A. Almers[b], T. El Bardouni[a], B. El Bakkari[a], E. Chakir[c]

[a] LMR/ERSN, Department of Physics, Faculty of Sciences, Abdelmalek Essaâdi University, B.P. 2121, Tétouan 93002, Morocco
[b] Department of Energetics, École Nationale Supérieure d'Arts et Métiers, Moulay Ismaïl University, B.P. 4024, Meknes, Morocco
[c] LRM/EPTN, Department of Physics, Faculty of Sciences, Kénitra, Morocco

ARTICLE INFO

Article history:
Received 15 August 2008
Received in revised form 30 December 2008
Accepted 18 January 2009

ABSTRACT

Over the last year (2007), preliminary tests have been performed on the Moroccan TRIGA MARK II research reactor to show that, under all operating conditions, the coolant parameters fall within the ranges allowing the safe working conditions of the reactor core. In parallel, a sub-channel thermal-hydraulic code, named SACATRI (Sub-channel Analysis Code for Application to TRIGA reactors), was developed to satisfy the needs of numerical simulation tools, able to predict the coolant flow parameters. The thermal-hydraulic model of SACATRI code is based on four partial differential equations that describe the conservation of mass, energy, axial and transversal momentum. However, to achieve the full task of any numerical code, verification is a highly recommended activity for assessing the accuracy of computational simulations. This paper presents a new procedure which can be used during code and solution verification activities of thermal-hydraulic tools based on sub-channel approach. The technique of verification proposed is based mainly on the combination of the method of manufactured solution and the order of accuracy test. The verification of SACATRI code allowed the elaboration of exact analytical benchmarks that can be used to assess the mathematical correctness of the numerical solution to the elaborated model.

1. Introduction

Thermal-hydraulic design and analysis is considered as an important aspect in safety studies of nuclear reactors. The role of such thermal-hydraulic analysis is to accurately predict the adequate working conditions, in steady state and transient conditions as well as in accidental situations, assuring the safe operation of nuclear reactors. Thermal-hydraulic analysis involves the determination of the optimal coolant flow distribution and the pressure drop between reactor core fuel assemblies. The mechanism of cooling of a reactor core depends rigorously on the amount of the heat generated by fuel elements. Most of power reactors, with important heat generation, are cooled by forced convection. Nowadays, several organisations are involved in the development of advanced reactors, operating at full power, using natural circulation for core cooling during normal operation (IAEA, 2005). However, natural circulation is widely adopted, as cooling mechanism, for research reactors having a relative small amount of heat generation. They present the feature of simplicity in the design of the reactor by eliminating pumps, power supplies, etc. The thermal response of natural circulation systems is sufficiently slow to give the reactor operator sufficient time to intervene to plant upsets.

For a detailed thermal-hydraulic simulation of nuclear reactors, a basic understanding of heat and mass transfer phenomena occurring between fuel assemblies is required. Thermal-hydraulic analysis of any system, cooled by natural convection, requires a detailed description of the physical phenomenon, accurate predictive tools, and validated benchmark data. In the last three decades, several codes have been developed to predict the thermal-hydraulic behaviour of nuclear reactors. They are classified into three categories. The first one, called System Codes, are based on lumped parameter approach. Widely used System Codes include ATHLET (Teschendorff et al., 1996; Austregesilo et al., 2003) and RELAP5/Mod3.3 (NUREG-5535, 2001). The second category is *sub-channel* codes. Some references code based on this approach are COBRA (Wheeler, 1976), MATRA (Yoo et al., 1999), and FLICA-4 (Toumi et al., 2000). The last category is Computational Fluid Dynamics (CFD) codes exemplified by FLUENT (FLUENT, 2005) and CFX (ANSYS, 2005).

During 2007, startup tests have been performed on the Moroccan TRIGA MARK II research reactor, operating at power level of 2000 kW. This category of reactors is the most widely used non-power nuclear reactor in the world cooled by natural convection. For a simplified thermal-hydraulic analysis, where the reactor core is represented by one-dimensional flow channel, some codes exist

* Corresponding author. Tel.: +212 79520291.
E-mail address: meroun.ossama@gmail.com (O. Merroun).

0029-5493/$ – see front matter © 2009 Elsevier B.V. All rights reserved.
doi:10.1016/j.nucengdes.2009.01.005

Nomenclature

A	flow area
a	coefficients in the discretized equation
a_n	coefficients of Taylor series expansions
Cp	heat capacity of the fluid
Err	discretization error
F	friction factor
g	gravitational acceleration
H	differential operator
h	enthalpy
h_0	reference enthalpy
N_k	number of adjacent sub-channels
φ	vector of unknowns variables
$\hat{\varphi}$	continuum solution function
P	pressure
Q	heat generation
$\bar{Q}$	grid refinement factor
q	grid size
r	order of accuracy
S	source term in the discretized equations
v	axial velocity
w	transversal velocity
ρ	coolant density
ρ_0	reference coolant density
v_{ik}	$0.5(v_i + v_j)$
Δx_{ik}	width of the gap between sub-channel i and k
Δy_{ik}	effective distance of interaction between sub-channel i and k
Δz	size of control volume in z direction
δ	Kronecker delta
ξ	transversal flow resistance coefficient
δP	pressure correction
β	thermal expansion coefficient

Subscripts

nb	neighbour nodal points
i	index of sub-channel i
j	index of the axial position of the sub-channels
k	index of sub-channel k
ik	index of the interface of two adjacent sub-channels i and k
P	main nodal points
a	exact solution
n	numerical solution

Superscripts

m	current iteration
m^*	previous iteration
**	value depending on the direction of the transversal cross-flow
*	value calculated at the interface of two adjacent sub-channels

as NCTRIGA (Smith, 1992) and TRISTAN (Mele, 1993). However, the tools for three-dimensional complex thermal-hydraulic simulation may not be readily available for some designs as the case of the Moroccan TRIGA MARK II research reactor. Consequently, the need to simulate the thermal-hydraulic behaviour of this reactor, with an acceptable degree of accuracy, has been satisfied by the development of Sub-channel Analysis Code for Application to TRIGA reactors code (SACATRI). In its first version, this code simulates the thermal-hydraulic behaviour of laminar single-phase flow between hexagonal and/or square lattices of TRIGA research reactors. We have used the sub-channel model (William, 1980; Macdougall and Lillington, 1984; Rowe, 1973) since it gives the most accurate practical representation of pin bundles. According to this approach, the reactor core is split into a number of vertical sub-channels exchanging one by one mass, momentum and energy.

To achieve the full task of any computational simulation, numerical codes used should reproduce accurately the experimental results. The process of comparing code predictions with experimental measurements is called *validation*. However, it is often difficult to obtain experimental data for various circumstances. Even if they exist, straightforward assessment of numerical results against experimental data could give, to code developers, confusing ideas about the uncertainty of code results. Almost all of the works realized in this field follow only the validation process to quantify the uncertainty of thermal-hydraulic codes (Jiang et al., 2007; Han et al., 2006; Toumi et al., 2000; Madeline and Miller, 1999; Veloso, 2004). The disadvantage of this process lies in the fact that the code can never be tested in a rigorous way. Generally, in numerous cases, the origin of the uncertainties detected by experimental validation can never be identified if they come from the discretization method used, the possible mistakes existing in the code or from different assumptions adopted in the physical model. Therefore, to satisfy an accurate simulation, *verification* activities are highly recommended before validation.

Recently, particular attention is given by the international scientific community concerning the subject of "Quantification of uncertainty" (Roache, 2002) involving verification and validation in computational science and engineering (Roache, 2002; Babuska and Oden, 2004; Oberkampf and Trucano, 2008; Roy, 2005). In fact, code validation differs from code verification. Validation addresses the physics modeling accuracy of computational simulation. In the other hand, verification is a purely mathematical exercise that examines the correctness of the numerical solutions. However, two aspects of verification can be defined in computational simulation: solution verification and code verification. The first one involves error estimation resulting from numerical simulation, whereas the second one involves error evaluation from known benchmark solution, bugs resulting from the programming of the code, the effectiveness of the algorithm solution, etc. The predefined terms, code verification, solution verification and validation have to be performed in this order, to warrant the effectiveness of quantifying uncertainties resulting from numerical simulation (Roache, 1998).

This study has been initiated with an aim to develop numerical benchmarks for verification of thermal-hydraulic codes based on sub-channel approach. For one-dimensional thermal-hydraulic simulation, it is possible to find benchmark tests allowing the verification of the code. In this case, an exact analytical solution of the problem can be easily obtained. Difficulties appear in three-dimensional problems when the governing thermal-hydraulic equations are strongly nonlinear and coupled on each sub-channel and between the adjacent ones through the inter-channel exchange of mass, momentum and energy. Relying on our experience (Merroun et al., 2007, 2008), mainly for this kind of problems that present some distinctions compared with standard CFD problems, the thermal-hydraulic code developer could finds enormous difficulties during the code development and verification activities. This is due to the lack of information in the literature concerning the detailed methods for solving the governing thermal-hydraulic equations and the accurate benchmarks with known analytical solutions, allowing a rigorous verification of the code.

The purposes of this paper are to (i) describe the mathematical model of SACATRI code and the numerical method used to solve the governing equations, (ii) to present the procedure of constructing numerical benchmarks allowing a rigorous verification of thermal-hydraulic codes based on sub-channel approach. The remainder

of the paper (Section 4) is devoted to describe the different steps followed to verify SACATRI code.

2. Development of SACATRI code

2.1. Natural flow circulation of TRIGA reactors

In most nuclear reactors, fuel elements are arranged in clusters of cylindrical rod bundles. The coolant is constrained to flow in parallel to the fuel pin from the bottom through orifices of the lower grid plates. It passes the unheated lower part of fuel element, the active section of the core, the upper axial reflector, the top end fixture, and leaves the channel through the holes in the upper grid plate. In natural circulation systems, as in the case of TRIGA research reactors, the fluid in contact with fuel element (heat sink) is being heated and its density decreases. Hence, the difference of density created in the reactor core, acted upon by gravity, produces a buoyancy force that drives the fluid through the channels of the reactor core. Fig. 1 illustrates the reactor core cooling mechanism via natural convection of TRIGA.

2.2. Mathematical model

As mentioned in the previous section, SACATRI code is based on the sub-channel approach. This approach is widely used in thermal-hydraulic analysis of nuclear reactors (Macdougall and Lillington, 1984; Veloso, 2004; Cheng et al., 2003). Using this approach, the reactor core is represented by different sub-channels physically bounded by cylindrical fuel rods. Fig. 2 shows different types of sub-channels that may exist for different TRIGA reactor cores. Thermal-hydraulic analysis is performed for an array of parallel sub-channels, discretized into axial intervals, delimited by planes normal to the z-axis (Fig. 3). The volumes bounded by the axial planes, the open gap and the fuel rod surfaces are assumed to receive coolant through their bottom inlet and from lateral interfaces. Axial velocity, pressure and enthalpy are calculated at the centre of each sub-channel i. Transversal velocities are defined at the interfaces separating adjacent sub-channels (Fig. 3). The thermal-hydraulic governing equations are solved in steady state regime. The basic equations of the model used in SACATRI code are summarized in the following subsections.

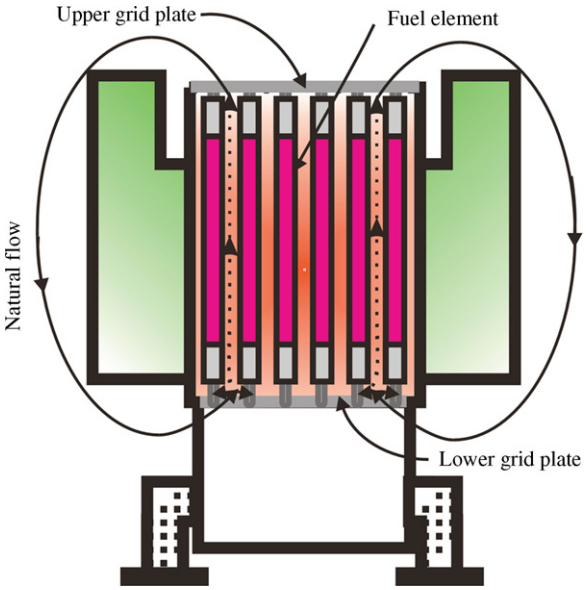

Fig. 1. Natural circulation cooling mechanism of TRIGA core.

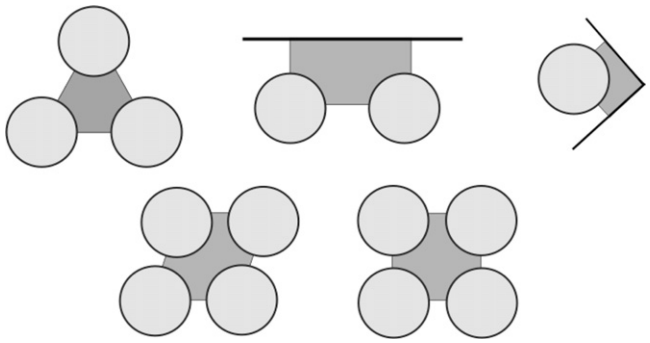

Fig. 2. Some sub-channel geometries of TRIGA research reactors.

2.2.1. Mass conservation equation

The mass balance applied to the control volume provides the continuity equation in the sub-channel i

$$\frac{\partial}{\partial z}(\rho_i v_i A_i) - \sum_{k=1}^{Nk} \rho_{ik} w_{ik} \ \Delta x_{ik} = 0 \tag{1}$$

Here N_k is the number of adjacent sub-channels. A, ρ, and Δx_{ik} denote the cross-section area of sub-channel i, the fluid density, and the width of the gap between sub-channel i and k, respectively. The second term represents the sum of transversal mass flow exchanged between the sub-channel i and the adjacent ones.

2.2.2. Axial momentum conservation equation

The conservation of axial momentum is given by the following equation:

$$\frac{\partial}{\partial z}(\rho v v A)_i - \sum_{k=1}^{Nk} (\rho_{ik} w_{ik} v_{ik}^{**}) \ \Delta x_{ik}$$

$$= -A_i \frac{\partial P_i}{\partial z} - g A_i(\rho_i - \rho_0) - A_i \frac{1}{2} F \rho_i |v_i| v_i \tag{2}$$

The terms on the left side of the axial momentum equation represent the axial and the transversal transport of axial momentum, respectively. The three terms on the right side are the gradient of pressure, body force and hydraulic resistance force. F denotes the friction factor and ρ_0 the fluid density at the reference temperature. The axial velocity v with asterisks (**) depends on the direction of the transversal flow. If the cross-flow is directed from the sub-channel k to i, then $v_{ik}^{**} = v_k$ ($w_{ik} > 0$). In the opposite case, we have $v_{ik}^{**} = v_i$. So, the second term of the left side of momentum equation

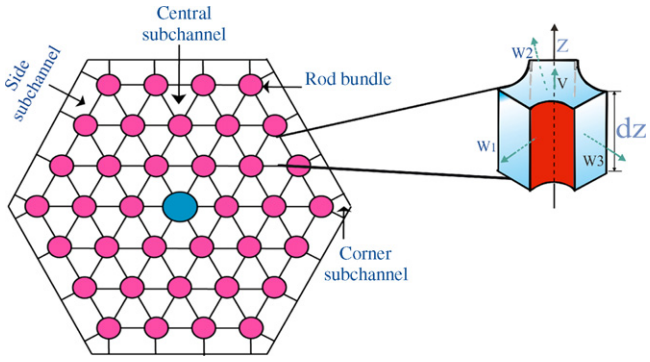

Fig. 3. Sketch of the sub-channel discretization and control volume of the reactor core.

can be rewritten as follows:

$$\sum_{k=1}^{Nk}(\rho_{ik}w_{ik}v_{ik}^{**})\,\Delta x_{ik}$$

$$=\sum_{k=1}^{Nk}(\rho_{ik}w_{ik}v_i)(1-\delta_{ik})\,\Delta x_{ik}+\sum_{k=1}^{Nk}(\rho_{ik}w_{ik}v_k)(\delta_{ik})\,\Delta x_{ik}$$

The Kronecker delta (δ) is zero when the flow is directed from the channel i to k, and equal to 1 when the flow is directed in the opposite direction.

2.2.3. Transversal momentum conservation equation

The inter-channel exchange of mass is described mainly through the pressure difference between two adjacent sub-channels. It can be written as follows:

$$\frac{\partial}{\partial z}(\rho\, w\, v^*)_{i\,k}=\frac{P_i-P_k}{\Delta y_{ik}}-\frac{\zeta_{i\,k}}{2\ \Delta x_{i\,k}}\rho_{ik}w_{i\,k}|w_{i\,k}| \tag{3}$$

where the left side term represents the axial transport of transversal momentum.

Here, k denotes the adjacent sub-channel, ξ is the transversal flow resistance coefficient of the gap between sub-channels i and k. Δy_{ik} is the effective distance of interaction between sub-channel i and k. The velocity v^* is calculated at the interface of the two adjacent sub-channels. Approximate value of v^* can be given by $v_{i\,k}^*=\frac{v_i+v_k}{2}$.

2.2.4. Energy conservation equation

The energy balance applied to the control volume, taking into account the heat Q_i that the sub-channel i receives from the fuel rods, leads to the following energy conservation equation:

$$\frac{\partial}{\partial z}(\rho v\, h\, A)_i-\sum_{k=1}^{Nk}(\rho\, w\, h^*)_{i\,k}\ \Delta x_{i\,k}=Q_i \tag{4}$$

Here, the inter-channel exchange of energy is caused only by the transversal mass flow represented by the second term at the left side of the energy conservation equation. The enthalpy h^* that appears in the second term is given by:

$$h_{i\,k}^*=h_k \text{ if } w_{i\,k}>0$$
$$h_{i\,k}^*=h_i \text{ if } w_{i\,k}<0$$

2.3. Boundary conditions

To solve the governing thermal-hydraulic equations, boundary conditions should be specified at the inlet and the outlet of each sub-channel. In this study, the diffusive terms are not retained. Hence, boundary conditions at the outlet of the assembly are not required. At the inlet of each sub-channel, enthalpy (or temperature) is imposed and assumed to be equal to the bulk coolant temperature in the reactor tank. To determine axial and transversal velocity values at the inlet of the fuel assembly, the pressure drop at the inlet of each sub-channel is used. Thereafter, correlations for the friction factors, as well as for the grid drag coefficients for localised pressure drop (due to the presence of spacer grids) are required.

2.4. Numerical solution and methods

2.4.1. Finite difference discretization

The predefined thermal-hydraulic equations are discretized using Finite Difference Method (FDM) using staggered Cartesian grids. Second-order central difference scheme is used to approximate convective and source terms. The SIMPLE algorithm (Patankar, 1980) is used to solve the pressure-velocity coupling. It is implemented by using an auxiliary pressure correction equation since there is no explicit form for this equation. Given a guessed pressure field P^*, axial and transversal velocity fields are obtained by solving the axial and transversal momentum equations:

$$(a_p^u v_p^*)_i=\sum(a_{nb}^u v_{nb}^*)_i+\frac{P_{i,j+1}^*-P_{i,j-1}^*}{2\ \Delta z}+S_i \tag{5}$$

$$(a_p^w w_p^*)_i=\sum(a_{nb}^w w_{nb}^*)_i+\frac{P_{i,j}^*-P_{k,j}^*}{\Delta y_{i\,k}} \tag{6}$$

The subscripts i and j indicate the considered sub-channel and the axial node, respectively. The velocity field may not satisfy the continuity equations. To enforce mass conservation, the velocities need to be corrected. This implies the correction of the pressure field. The equation of pressure calculation is obtained on the basis of continuity equation. To eliminate the velocity components from continuity equation, the expressions for calculating the velocity correctors are substituted into the continuity Eq. (1) where δP is the pressure correction

$$v_i=v_i^*+\frac{\delta\, t}{\rho}\frac{\partial\,\delta P}{\partial z} \tag{7}$$

$$w_i=w_i^*+\frac{\delta t}{\rho}\left(\frac{\delta P_i-\delta P_k}{\Delta y_{i\,k}}\right) \tag{8}$$

By replacing Eqs. (7) and (8) into the continuity Eq. (1), a Poisson type equation for calculating the pressure correction is obtained. The field of pressure is obtained using the following expression $P^m=P^{m^*}+\delta P^m$ where m and m^* indicate respectively the current and the previous iteration. Here δt is selected in order to improve the convergence of the iteration process.

2.4.2. Numerical flow chart

Fig. 4 shows the numerical flow chart adopted in SACATRI code, to solve the governing thermal-hydraulic equations. The solution procedure starts by assuming an initial guess of pressure and velocity field. Then, axial and transversal momentums are solved to obtain a temporary velocity fields. The new velocities are incorporated into the pressure correction equation to obtain the pressure corrections. Finally, temporary velocities and pressure are updated based on the velocities corrections equations (Eqs. (7) and (8)). Those steps are repeated until the momentum and pressure correction equations reach the required accuracy. However, an outer loop is required to sweep iteratively all the sub-channels of the reactor core.

3. Verification activities

To satisfy an accurate simulation, verification tests are very recommended activities. Relying on the work of Oberkampf and Trucano (2002), it is useful to separate the verification procedure into two activities: numerical algorithm verification and software quality engineering (SQE). The first one deals with assessing the difference between simulation results of a given problem, and the corresponding mathematical model. The major goal of numerical algorithm verification is to demonstrate that, the numerical algorithm used is implemented correctly and working as intended (Oberkampf and Trucano, 2008). The second activity (SQE) is focussed on determining the reliability of the code and its capability to produce the same results on specified computer hardware and under specified software environment. More details about SQE activity are explained in the works of Oberkampf and Trucano (2008), Roy (2005) and Christensen and Thayer (2001). In this study, emphasis on verification activities is given. We try to present the most important steps that thermal-hydraulic sub-channel code

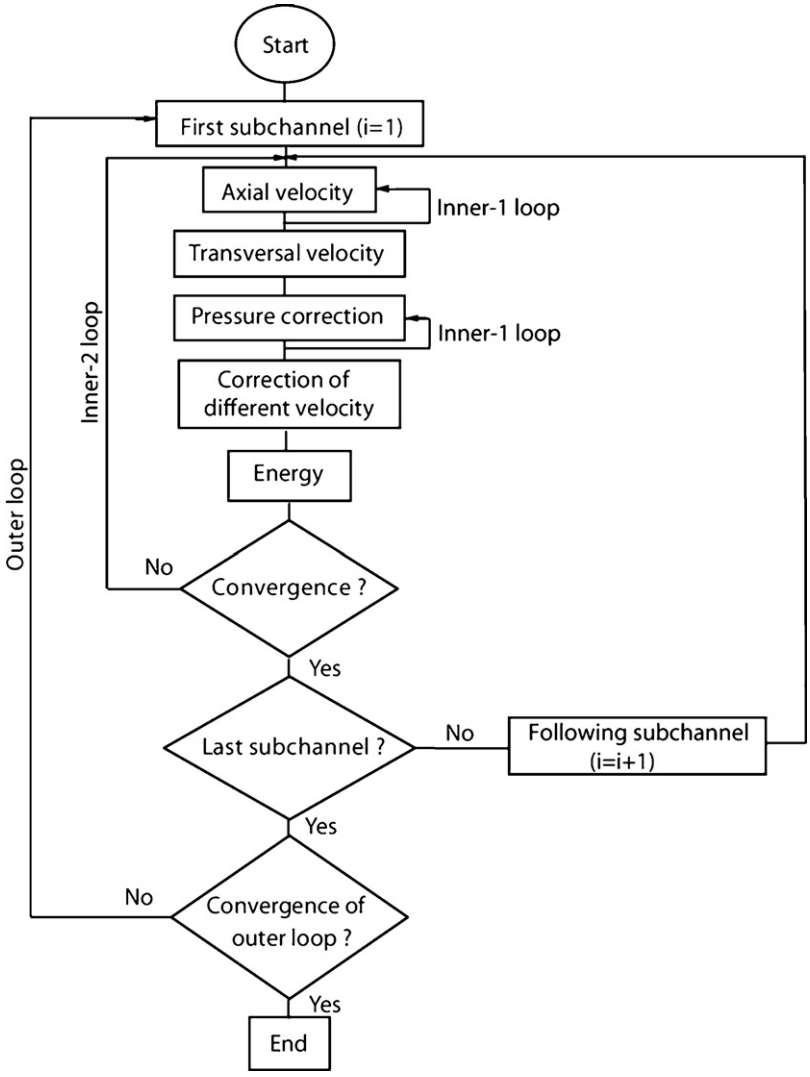

Fig. 4. Numerical flow chart of SACATRI code.

developer could proceed to verify the efficiency of the numerical algorithm used.

3.1. Code verification procedures

For code verification activities, several approaches can be used to assess the reliability and the correctness of computer codes. Each approach gives to the developers and users of numerical codes a clearer idea about the accuracy of simulation results. Some straightforward verification tests are based on: (1) the use of benchmark solutions that could exist in the literature or calculated with a high degree of accuracy; (2) code to code comparison. The last verification test is inadvisable, since a code cannot be verified rigorously by a simple comparison to an unverified code. However, detecting source of errors during the code verification involves the development of highly accurate verification benchmarks, which the solution should be mathematically assessed.

Oberkampf and Barone (2004) as well as AIAA guide (AIAA, 1998) suggest the employment of an exact analytical solutions considered as a highly accurate benchmark solutions. For one-dimensional thermal-hydraulic problems, an analytical solution can be easily obtained. Difficulties arise in simulating three-dimensional problems, where the governing thermal-hydraulic equations are strongly nonlinear and coupled on each sub-channel and between the adjacent ones via the inter-channel exchange of mass, momentum and energy. Hence, to find analytical solutions, we have used a powerful approach for code verification based on the Method of Manufactured Solution (MMS). This method proposed by Roache (1998) provides a general procedure for constructing an analytical solution for code accuracy verification. MMS has proved that it is very sensitive to mistakes resulting from discretization, and allows testing different options related to the numerical solution of PDEs. Unfortunately, MMS could not detect the coding mistakes that affect the efficiency of the numerical algorithm implemented into the code. However, the most rigorous code verification test is based on the examination of the Observed Order of Accuracy (OOA). The aim of using this test is to verify that the observed order of accuracy obtained from numerical results, agree with the order of accuracy calculated theoretically. In what follow, we will discuss in more detail, the principle of MMS and the order of accuracy test used for verification of SACATRI code.

3.1.1. Method of manufactured solution

The method of manufactured solution is a general procedure that can be used to construct analytical solutions to the PDEs. Since the verification is a purely mathematical exercise, manufactured

solutions can be generated with no concern whatever for the accuracy of physical laws. Application of MMS consists in choosing a continuum solution function $\hat{\varphi}$ that can be virtually independent of the PDEs (Roache, 2002). The selected solution should be differentiable function allowing a full description of the desired evolution of the variables in space and time. In other words, the choice of non-trivial but analytical solution must exercises all derivative terms.

For example, let us consider a generic system of differential equations $H(\varphi)=0$ where φ is a vector of unknown variables and $H(\varphi)$ is a differential operator whose specific form depends on the PDEs. Since $\hat{\varphi}$ does not necessary satisfy the original governing equations, a corresponding set of source terms S_φ are generated by applying the differential operator to $\hat{\varphi}$ in order to balance the following system:

$$H(\hat{\varphi}) = S_\varphi \tag{9}$$

The new equations deduced from Eq. (9) constitute an exact analytical solution that exercises all of the same differential terms as $H(\varphi)=0$. Consequently, Eq. (9) can be used to test numerical codes designed to solve the original equations $H(\varphi)=0$ with minimal additional coding.

Boundary conditions can be easily obtained from the manufactured solutions. MMS allows testing different type of boundary. So, one can use the chosen solution function to: (1) evaluate Dirichlet boundary conditions; (2) Neumann type boundary conditions; and (3) third kind boundary conditions obtained analytically from both the solution function value and its derivative.

Because MMS involves the incorporation of each manufactured solution and source terms in the computer code, it is preferable to apply MMS at the time of the code development to avoid the disturbing of the code, or non-desirable numerical problems that could affect the numerical results. More detailed discussions about the method of manufactured solution can be found in the book published by Knupp and Salari (2002). The implementation of MMS for verifying SACATRI code will be explained with more in Section 4.

3.1.2. Evaluation of the order of accuracy

The evaluation of the observed order of accuracy (OOA) is a rigorous test, which determines whether of not the discretization error is reduced at the expected rate (Roy, 2005). By calculating the observed order of accuracy, one can verify if the code converges to the correct solution or not. If the OOA matches or nearly matches the formal order of accuracy, the code is considered able to reproduce the formal order of accuracy (FOA) of the numerical method. Hence, the code can converge to the correct solution.

The evaluation of the FOA can be illustrated through the following example, using the energy equation used in SACATRI code. FOA is determined by evaluating the truncation error using Taylor series expansion of the solution variable(s).

For a single sub-channel, the energy equation is written as:

$$\frac{\partial}{\partial z}(\rho v h A)_i - \sum_{k=1}^{Nk}(\rho w h^*)_{ik}\,\Delta x_{ik} = Q_i$$

To simplify this equation, we adopt the following assumptions:

(i) $w_{ik} > 0$ which implies that $h^*_{ik} = h_k$.
(ii) The fluid density (ρ) and the velocity (v) are supposed constant.
(iii) Transversal velocities are the same at the three sides of the sub-channel

$$\sum_{k=1}^{Nk=3}(w)_{ik} = w_{i1} + w_{i2} + w_{i3} = 3w_{ik} = w$$

Taking into account the continuity equation, the energy conservation equation becomes:

$$\frac{\partial h_i}{\partial z} = S_i \text{ where } S \text{ is the source term.}$$

Using central difference scheme, the finite difference discretization of the energy equation leads to the following discretized form:

$$\frac{(h_i)_{j+1} - (h_i)_{j-1}}{2\Delta z} = S_i \tag{10}$$

The subscript j denotes the axial node location. Developing a Taylor series expansion for $h(z_0+\Delta z)$ and for $h(z_0-\Delta z)$ about (z_0) gives

$$\begin{aligned}(h_i)_{j+1} &= h_i(z_0+\Delta z)\\ &= h_i(z_0) + \left.\frac{\partial h_i}{\partial z}\right|_0 \Delta z + \left.\frac{\partial^2 h_i}{\partial z^2}\right|_0 \frac{(\Delta z)^2}{2!} + \left.\frac{\partial^3 h_i}{\partial z^3}\right|_0 \frac{(\Delta z)^3}{3!} + O(\Delta z^4),\end{aligned} \tag{11}$$

$$\begin{aligned}(h_i)_{j-1} &= h_i(z_0-\Delta z)\\ &= h_i(z_0) - \left.\frac{\partial h_i}{\partial z}\right|_0 \Delta z + \left.\frac{\partial^2 h_i}{\partial z^2}\right|_0 \frac{(\Delta z)^2}{2!} - \left.\frac{\partial^3 h_i}{\partial z^3}\right|_0 \frac{(\Delta z)^3}{3!} + O(\Delta z^4),\end{aligned} \tag{12}$$

Substituting expressions (11) and (12) into the discretized equation (10) we obtain

$$\frac{\partial h_i}{\partial z} = \frac{(h_i)_{j+1} - (h_i)_{j-1}}{2\ \Delta z} - \left[\frac{1}{6}\frac{\partial^3 h_i}{\partial z^3}\right](\Delta z)^2 + O(\Delta z^4) = S_i. \tag{13}$$

The term $\left[\frac{1}{6}\frac{\partial^3 h_i}{\partial z^3}\right](\Delta z)^2 + O(\Delta z^4)$ represents the truncation error. It tends to zero when Δz goes to zero. So, the formal order of accuracy of the scheme is second order because the truncation error term contains the factor $(\Delta z)^2$.

The observed order of accuracy is directly calculated from simulation results. If an analytical solution exists, the observed order of accuracy is determined by using the discretization error calculated using two resolution meshes. The discretization error is the difference between numerical and analytical solution. For this case, the OOA can be calculated as follows (Shyy et al., 2002):

Let us consider a series of the form given below for a grid size q, then:

$$\phi_a(x) = \phi_n(x;q) + a_2q^2 + a_3q^3 + a_4q^4 + \ldots \tag{14}$$

$\phi_a(x)$ is the exact solution and $\phi_n(x;q)$ is the numerical solution based on q. The corresponding discretization errors can be written as:

$$\phi_a(x) - \phi_n(x;q) = a_2q^2 + a_3q^3 + a_4q^4 + \ldots$$

Using the first or second order discretization scheme, the higher-order terms can be neglected witch implies that the solutions are in the asymptotic region:

$$\phi_a(x) - \phi_n(x;q) = a_2q^2 + O(q^3)$$

Or simply

$$Err(x) = |\phi_a(x) - \phi_n(x;q)| = |a_2|q^2 \tag{15}$$

This expression of error discretization can be rewritten, for a given coarse (q_1) and fine (q_2) mesh, as

$$Err_1(x) = |\varphi_a(x) - \varphi_{n_1}(x;q_1)| = |a_2|q_1^2$$

and

$$Err_2(x) = |\phi_a(x) - \phi_{n_2}(x;q_2)| = |a_2|q_2^2$$

Then we have

$$\frac{Err_2(x)}{Err_1(x)} = \left(\frac{q_2}{q_1}\right)^r = (\bar{Q})^r$$

$\bar{Q}$ is the grid refinement factor. From this relation the order of accuracy r is equal to 2. In general, the observed order of accuracy can be written as:

$$r = \frac{\ln(Err_2(x)/Err_1(x))}{\ln(\bar{Q})} \tag{16}$$

In this case, where analytical solution exists, the observed order of accuracy is evaluated using only the numerical solution over two resolution meshes. At this stage, MMS is applied to generate analytical solution only for a limited number of sub-channels, since the symbolic manipulation of all derivative terms becomes a very complicated procedure if the number of sub-channel becomes important. In this case, the estimation of the observed order of accuracy can be carried out by using three different numerical solutions on three different grid sizes.

For example, the observed order of accuracy, where the grid is refined by a factor of 2($\bar{Q} = 2$), can be calculated as follow:

$$\bar{Q} = \frac{q_2}{q_1} = \frac{q_3}{q_2} = 2$$

q_1, q_2 and q_3 represent respectively the coarse, medium and fine meshes. This can be rewritten in an another form as follows:

$$q_1 = f, \quad q_2 = 2f, \quad q_3 = (2)^2 f$$

Then, by neglecting higher-order terms, the three discretization error equations can be written as

$$\phi_{n1}(x; q_1) = \phi_a(x) + a_2 f^r + \dots$$
$$\phi_{n2}(x; q_2) = \phi_a(x) + a_2 (2f)^r + \dots$$
$$\phi_{n3}(x; q_3) = \phi_a(x) + a_2 ((2)^2 f)^r + \dots$$

Then, the observed order of accuracy r is given by the relation:

$$r = \frac{\ln(\phi_{n3} - \phi_{n2}/\phi_{n2} - \phi_{n1})}{\ln(\bar{Q})} \tag{17}$$

3.2. Solution verification

After code verification, it is very important to estimate the accuracy of the numerical results obtained by computer codes. The solution verification activities depend strongly on the correctness and completeness of the code verification activities. The numerical solutions can be affected by several sources of numerical errors. The most encountered errors are: (1) round-off error due to the use of finite arithmetic on digital computers; (2) iterative convergence error that often exists when resolving, iteratively the nonlinear PDEs; and (3) discretization error. The first and second source of numerical errors is often neglected compared to discretization errors. For solution verification of SACATRI code, emphasis is given to estimate numerical errors resulting from discretization of the governing thermal-hydraulic equations.

The discretization error is defined as the difference between the numerical and the exact solution to the continuum PDEs. The relative discretization error (RDE) is the difference between the numerical solution and the exact solution normalised by the exact solution. RDE can be written as

$$\mathrm{RDE}_\phi = \frac{\phi_n - \phi_a}{\phi_a} \tag{18}$$

ϕ represents the different variables of the problem. If the formal order of accuracy is $r = 2$, and the grid is refined by a factor of two ($\bar{Q} = 2$), the discretization error for 4 resolution meshes should obeys in the asymptotic grid region, to the following relationship:

$$\mathrm{RDE}_{q_{1\phi}} = \mathrm{RDE}_{q_{2\phi}}(\bar{Q}^p) = \mathrm{RDE}_{q_{3\phi}}(2\bar{Q})^p = \mathrm{RDE}_{q_{4\phi}}(4\bar{Q})^p \tag{19}$$

For unknown analytical solutions and if the numerical scheme used is second order accurate and the grid is refined by a factor of two, standard Richardson extrapolation (Roy, 2005) can be used to estimate the exact solution as follows:

$$\phi_a = \phi_2 + \frac{\phi_2 - \phi_1}{3} \tag{20}$$

ϕ_1 and ϕ_2 are the numerical solutions in coarse and fine mesh, respectively. In this case ϕ_a is third order accurate solution. Generalised form of Richardson extrapolation can be given by:

$$\phi_a = \phi_1 + \frac{\phi_1 - \phi_2}{\bar{Q}^r - 1} \tag{21}$$

By using Eqs. (18) and (21), the discretization error estimator (using Richardson extrapolation) is given by:

$$\mathrm{RDE}_{1\phi} = \frac{\phi_2 - \phi_1}{\phi_{\mathrm{exact}}(\bar{Q}^r - 1)} \tag{22}$$

4. Verification of SACATRI code

In this section, we discuss the procedure that can be envisaged to verify thermal-hydraulic codes based on the sub-channel approach. To simplify the problem, the procedure of verification will be subdivided into three stages. In the first one, we consider a single sub-channel with imposed transversal velocities. In this case, the transversal momentum equation cannot be used, because the transversal velocities are known. In the second stage, we consider a central sub-channel surrounded by three others ones. The inter-channel exchange of mass, energy and momentum is carried out through the three interfaces of the central sub-channel. This situation is envisaged for the verification of the inter-channel exchange of mass, momentum and energy. In the last step, we will verify the code in a case closer to the reality, where the thermal-hydraulic equations are solved for an array of sub-channels using real geometrical and physical data.

4.1. Single sub-channel with imposed transversal flows

Let us consider a single triangular sub-channel which is assumed to receive lateral flows from its three interfaces (Fig. 5). The following transversal velocities are imposed:

$$w_{i1}(z) = w_{i2}(z) = w_{i3}(z) = w(z); \qquad (w > 0)$$

In this case, terms corresponding to transversal heat and mass flux will not be verified. For simplifying the problem, Boussinesq's hypothesis is used. This approach implies that the fluid density (ρ) is constant except in the term corresponding to the Archimedes forces in the axial momentum equation. ρ can be expressed as:

$$\rho = \rho_0 + \beta T \tag{23}$$

To generate an exact analytical solution, MMS has been applied to the governing thermal-hydraulic equations. In this case, the manufactured solution for enthalpy and axial velocity is chosen as

$$h(z) = h_0 e^{\alpha z} \tag{24}$$

$$v(z) = v_0 + b \sin(\omega z) \tag{25}$$

Here, h_0 and v_0 are the enthalpy and the velocity at the inlet of the sub-channel. The constants α, b and ω are chosen to take into account the simplicity of the analytical form and to retain the same degree of complexity after derivation.

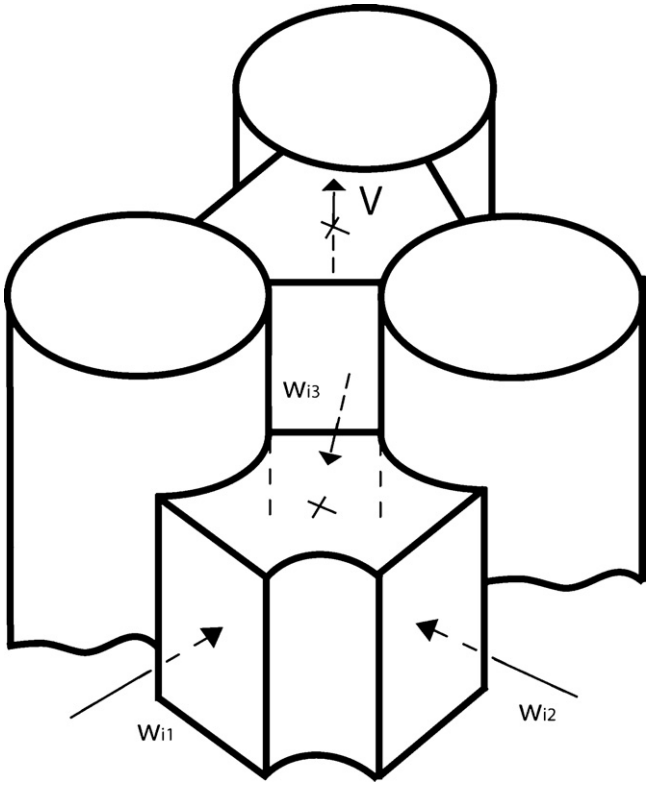

Fig. 5. Sketch of a single sub-channel with imposed transversal velocities.

The analytical form of the transversal velocity must satisfy the mass conservation equation. By Substituting $v(z)$ into the continuity Eq. (1), the analytical form of transversal velocity is given by:

$$w_{ik}(z) = \frac{A\,b\,\omega}{3\,\Delta x_{ik}}\,\cos(\omega z) \tag{26}$$

Substitution of the chosen manufactured solutions into the energy equation allows the analytical form of the source term Q. Then we have

$$Q(z) = \rho A \alpha h_0 (v_0 + b\,\sin(\omega z)) e^{\alpha z} \tag{27}$$

The analytical form of the pressure field is obtained by integrating the axial momentum Eq. (3). The friction factor F is represented by an exponential function $F(z) = e^{\lambda z}$ where λ is a constant parameter.

The analytical pressure field is given by:

$$P(z) = -2\rho b\left(v_0 + \frac{b}{2}\,\sin(\omega z)\right)\sin(\omega z) - \left(\frac{g\beta}{\alpha Cp}\right)h(z)$$
$$-\frac{\rho A}{2}\int e^{\lambda z} v^2(z)dz + \rho\beta\omega\int v(z)\,\cos(\omega z)dz + P_0 \tag{28}$$

where P_0 is a constant resulting from the integration of the axial momentum equation. It is defined by the boundary conditions.

Finally, the present test problem can be described by: (1) boundary conditions, (2) source term of the energy conservation equation and (3) the analytical transversal velocity. Q and w are incorporated into SACATRI code. Parameters used in our simulation for this verification test are presented in Table 1.

$$\begin{aligned} z = 0: \quad & h = h_0 \\ & v = v_0 \\ 0 \le z \le L: \quad & w_{ik}(z) = \frac{A\,b\,\omega}{3\,\Delta x_{ik}}\sin(\omega z) \\ & Q(z) = \rho A \alpha h_0 (v_0 + b\sin(\omega z)) e^{\alpha z} \end{aligned}$$

Table 1
Parameters used in the first verification test.

L (m)	0.7
h_0 (kJ/kg)	134.11
v_0 (m/s)	0.1
A (m^2)	2.67E−4
Δx_{ik} (m)	0.0435
b	0.1
ω	2.2341
α	60
β	6.73E−2

Table 2
Meshes employed in the evaluation of the observed order of accuracy and relative discretization error.

Mesh name	Mesh nodes	Grid spacing, q
N_1	20	$(N_5/N_1) = 8$
N_2	40	$(N_5/N_2) = 8$
N_3	80	$(N_5/N_3) = 4$
N_4	160	$(N_5/N_4) = 2$
N_5	320	–

Table 3
Relative discretization error for enthalpy (h), axial velocity (v) and pressure (P).

Mesh nodes	RDE$_h$	RDE$_v$	RDE$_P$
20	1.5110E−01	4.0295E−02	2.9225E−01
40	3.7829E−02	9.6414E−03	7.2622E−02
80	9.4559E−02	2.3591E−03	1.8058E−02
160	2.3629E−03	5.8460E−04	4.5132E−03

The estimation of the numerical discretization errors has been performed for regular meshes in the axial direction where the grid refinement factor is equal to 2. The meshes employed are summarized in Table 2. Results of the RDE$_\varphi$ and the observed order of accuracy (r_φ) as a function of the element size q are presented in Table 3 and Fig. 6, respectively.

The profiles of different parameters compared to the analytical solution for different mesh resolutions are presented in Figs. 7, 8 and 9.

It is noted that the analytical and the numerical solution agree perfectly for different mesh resolutions. The difference between the exact and the numerical solution cannot be noted on the figures. This is explained by the fact that even for coarser grid mesh ($N_1 = 20$) the relative error for all parameters is less than 0.3% (Table 3). This error is systematically reduced when the node size increases.

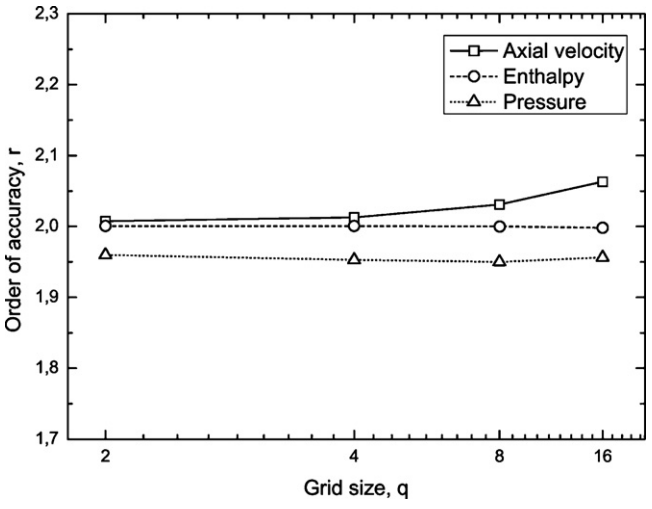

Fig. 6. Observed order of accuracy for axial velocity, enthalpy and pressure.

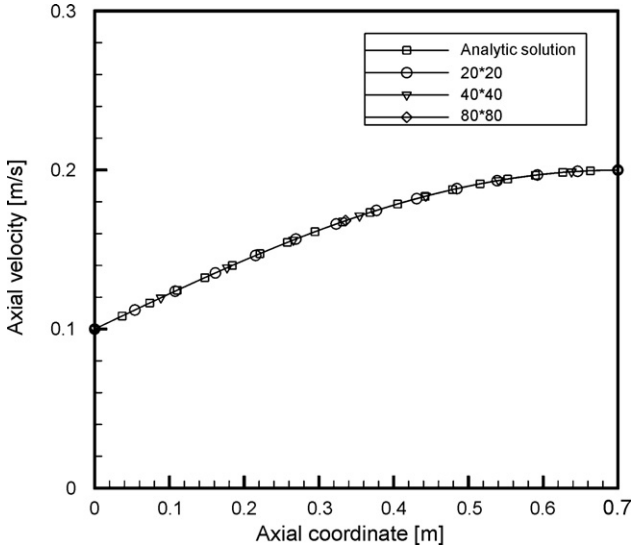

Fig. 7. Axial velocity profile for different node size and compared to the analytical solution.

As can be seen from Fig. 6, the observed order of accuracy of the solution (averaged value obtained over all nodes for a given resolution mesh) generally agrees with the theoretical one. This is due to the fact that the central finite difference scheme (second order) is applied in all nodes of the calculation domain. Here a special attention should be taken during the numerical treatment of the boundary conditions, because if it is evident to apply the second-order central difference scheme at internal nodes, this is not the same thing for the nodes corresponding to the boundary conditions. Mainly for the last node corresponding to the outlet of the sub-channel, the application of the central finite difference scheme requires an additional node (physically exists at the external of the calculation domain). Subsequently, for the code developer, the convenient solution can be the use of a backward finite difference scheme (first order). In this case, the verification results can be not clear or erroneous because the calculated observed order of accuracy is near 1. In our code this problem was solved by using the central finite difference scheme applied by considering an auxiliary node located between the two last nodes of the computational domain.

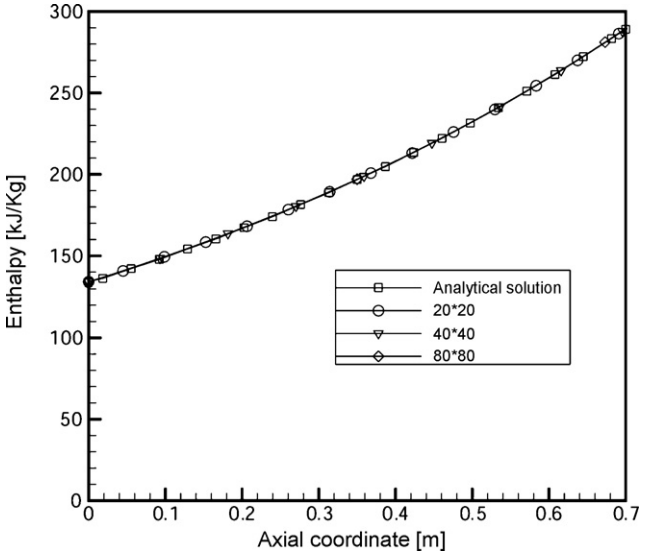

Fig. 8. Enthalpy profile for different node size and compared to the analytical solution.

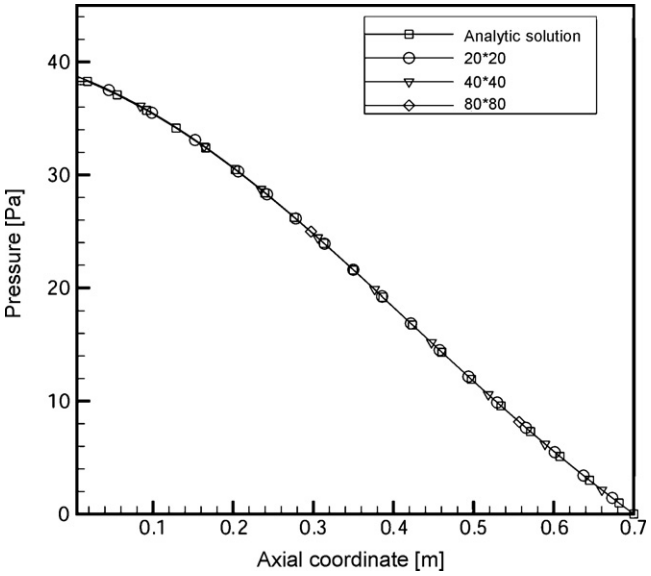

Fig. 9. Pressure profile for different node size and compared to the analytical solution.

However, for the pressure field, the averaged observed order of accuracy is slightly less than the formal one ($r=2$). For the pressure correction equation, the averaged observed order of accuracy is affected by the numerical treatment of the boundary conditions, mainly at the inlet of the sub-channel. Indeed, the pressure correction equation is not one of the governing equations and its boundary conditions cannot be obtained explicitly from the physical problem. In general, whatever the boundary conditions imposed on the pressure correction equation, this equation must ensure that the velocities in the entire flow field satisfy the continuity equation. In the inlet of the sub-channel ($z=0$) the axial velocities are known, so the axial velocity correction equation indicates that it is not necessary to correct the gradient of pressure. Then we have:

$$\frac{\partial \delta P}{\partial z} = 0 \tag{29}$$

This boundary condition is implemented by a forward finite difference scheme (first order), because the use of the central finite difference scheme (second order) in this case provokes the disturbances in the iterative process. Subsequently, the observed order of accuracy for the pressure field at the inlet ($z=0$) is equal to 1. This value affects the averaged order of accuracy for the pressure correction equation over the calculation domain. The influence of this effect is deadened in the axial momentum equation which uses only the pressure gradient (explicitly known at the inlet of the sub-channel).

4.2. Central sub-channel surrounded by three adjacent ones

In this test we consider a central sub-channel surrounded by three adjacent ones. The inter-channel exchanges of mass, energy and momentum are considered as shown in Fig. 10. The following simplifications are adopted: (i) sub-channels 2, 3 and 4 have the same boundary conditions and source terms in the energy equation, (ii) transversal mass flows at the external interfaces of the three adjacent sub-channels (2, 3 and 4) are null, and (iii) the central sub-channel receives transversal mass flows from the three adjacent ones. The symmetry considered in this case cannot affect numerically the quality of the test problem, because the test can exercise all derivative terms in the partial differential equations. The MMS is applied through the following steps.

4.2.1. Central sub-channel i

In the central sub-channel i we propose the following analytical solution for enthalpy and transversal velocity.

$$h_i(z) = h_0 e^{\alpha z} \tag{30}$$

$$w_{ik}(z) = \frac{A}{3\ \Delta x} e^{-kz} \cos(\omega z) \tag{31}$$

Substitution of the chosen manufactured solutions into the continuity and the energy equation allows the analytical determination of the axial velocity v_i and the source term Q_i, respectively.

$$v_i(z) = -\frac{e^{-kz}}{k^2+\omega^2}(k\ \cos(\omega z) - \omega \sin(\omega z)) + v_0 \tag{32}$$

$$Q_i(z) = \rho A[\alpha h_0 v_i(z) e^{\alpha z} + (h_0 e^{(\alpha-k)z} - h'_0 e^{(\alpha'-k)z})\ \cos(\omega z)] \tag{33}$$

4.2.2. Sub-channels k (k = 2, 3 and 4)

For the three adjacent sub-channels, we have $w_{ki} = -w_{ik}$ (the mass flow is directed from the sub-channel i to the sub-channels k), then we have:

$$w_{ki}(z) = -\frac{A}{3\ \Delta x} e^{-kz} \cos(\omega z) \tag{34}$$

Introducing this equation into the equation of continuity yields:

$$v_k(z) = \frac{e^{-kz}}{3(k^2+\omega^2)}(k\ \cos(\omega z) - \omega \sin(\omega z)) + v'_0 \tag{35}$$

The analytical form proposed for enthalpy h is expressed as:

$$h_k(z) = h'_0 e^{\alpha' z} \tag{36}$$

Substituting the chosen analytical solutions into the energy conservation equation gives the following source term in the energy equation:

$$Q_k(z) = \rho A \alpha' h'_0 v_k(z) e^{\alpha' z} \tag{37}$$

As mentioned above, the transversal mass flow is directed from the sub-channels (k) to the central sub-channel (i). Physically, the pressure in the central sub-channel must be less than the pressure in the adjacent ones. However, there is no constraint imposed on the transversal momentum equation verifying this condition on the pressure because at this stage the transversal momentum equation is never used to evaluate the analytical form of the thermal-hydraulic variables of the problem. Mainly, the parameter ζ appears only in the transversal momentum equation, then, for two different values of ζ we have two different solutions. Subsequently, to close the system of equations, we must evaluate the form of ζ that correspond to our analytical solution already specified. This analytical form can be easily obtained from Eq. (3).

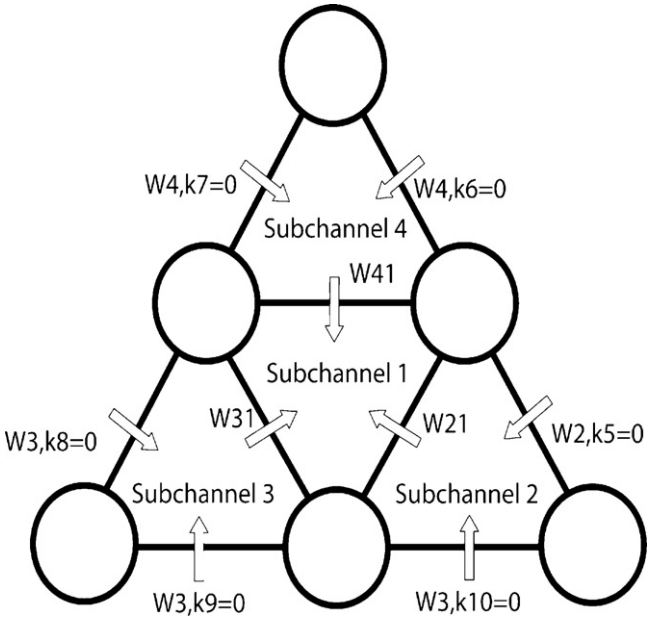

Fig. 10. Arrangement of four sub-channels.

Table 4
Parameters used in the second verification test.

h_0 (kJ/kg)	134.11
h'_0 (kJ/kg)	157.89
v_0 (m/s)	0.3
v'_0 (m/s)	0.1
b	2
ω	2.2341
α	1.1
α'	0.9
k	5

Since the thermal-hydraulic governing equations are solved via an iterative procedure, it is preferable, from the point of view of convergence, to update ζ in each iteration. Thus, based on the transversal momentum equation, we have used the following expression for ζ:

$$\zeta_{ik}(z) = \frac{1}{w^*_{ik}} \left[\frac{2\ \Delta x_{ik}}{\rho |w_{ik}|} \left(\frac{P_i - P_k}{\Delta y_{ik}} - \frac{\partial(\rho v^* w)_{ik}}{\partial z} \right) \right] \tag{38}$$

In this equation only w^* is updated during the iteration procedure. The analytical expression of the terms between the square brackets is expressed directly by using the analytical form of different variables. The obtained value of the coefficient ζ_{ik} cannot have any physical signification, because it used only to balance the equation of transversal momentum.

The different parameters used for this verification test are summarized in Table 4. Figs. 11–14 illustrate, for different node size, the profiles of the calculated thermal-hydraulic parameters compared to the analytical solution. The agreement observed between both numerical and analytical solutions is adequate even for the coarsest grid. The RDE for axial and transversal velocities, enthalpy and pressure field are presented in Table 5. In general, the RDE for all variables of the problem is less than 0.5%, and it is reduced systematically when the node size increases.

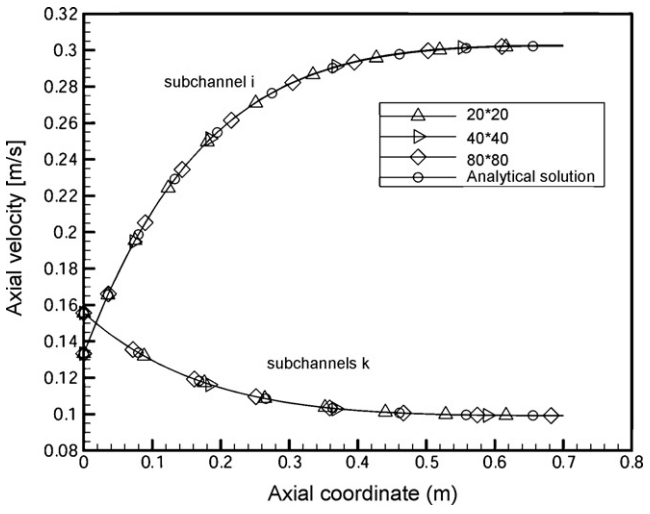

Fig. 11. Axial velocity profile in the sub-channel i and sub-channels k (k = 1, 2 and 3) for different node size and compared to the analytical solution.

Table 5
Relative discretization errors for enthalpy (h), axial and transversal velocities (v and w) and for pressure field (P).

Mesh nodes	20		40		80		160	
	i	k	i	K	I	k	I	K
RDE_h (%)	2.89E−1	2.04E−2	7.34E−2	5.22E−2	1.84E−2	1.31E−2	4.62E−3	3.31E−3
RDE_v (%)	1.41E−1	1.26E−1	3.38E−2	3.03E−2	8.29E−3	7.42E−3	2.04E−3	1.83E−3
RDE_w (%)	7.68E−2	7.68E−2	1.79E−2	1.79E−2	4.13E−3	4.13E−3	9.91E−4	9.91E−4
RDE_P (%)	5.08E−1	4.85E−1	1.29E−1	1.24E−1	3.27E−2	3.18E−2	8.31E−3	8.03E−3

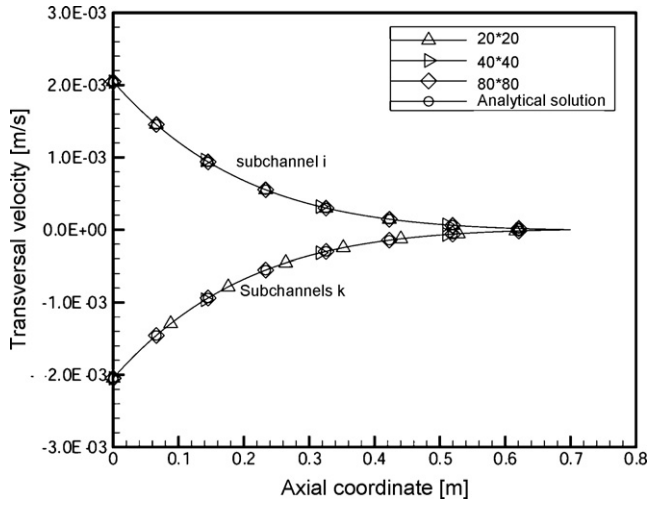

Fig. 12. Transversal velocity profile in the sub-channel i and sub-channels k (k = 1, 2 and 3) for different node size and compared to the analytical solution.

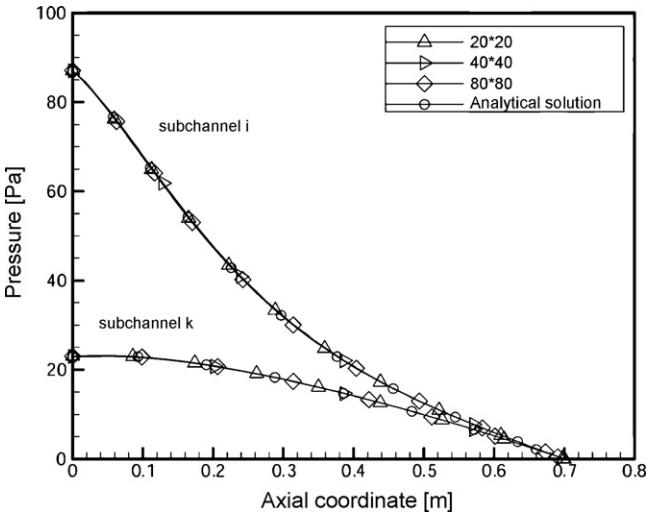

Fig. 14. Pressure profile in the sub-channel i and sub-channels k (k = 1, 2 and 3) for different node size and compared to the analytical solution.

Fig. 15 presents the averaged observed order of accuracy calculated for axial and transversal velocities, enthalpy and pressure field. The Results show a good agreement between the observed order of accuracy and the theoretical one. However, for the same reasons previously cited in the last verification test, the order of accuracy corresponding to the pressure correction equation, is slightly less than the formal one.

4.3. Parameters affecting the OOA

If the code developer finds some disagreements between the observed and the formal order of accuracy, the origins of these disagreements can be divers, the more frequents can be summarized as follows: (1) Programming errors or bugs existing in the code; (2) Inadequate numerical treatment of the boundary conditions; (3) The grid size is insufficient and the solution is note in the asymptotic convergence region; (4) inadequate convergence of the iterative procedure. Some references in these topics can be found: Oberkampf and Trucano (2008), Botella and Peyret (2001), and Knupp and Salari (2002).

Concerning the convergence quality of the iterative procedure, a special attention must be taken, because the observed order of accuracy can be erroneous if the iterative process cannot converge sufficiently. Indeed, as shown in Fig. 4, two levels of iterations are required in SACATRI code. In the inner level (inner-2 loop), based on

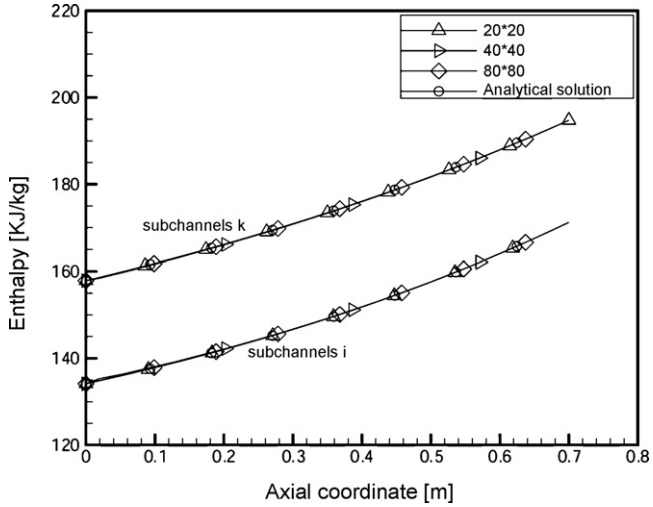

Fig. 13. Enthalpy profile in the sub-channel i and sub-channels k (k = 1, 2 and 3) for different node size and compared to the analytical solution.

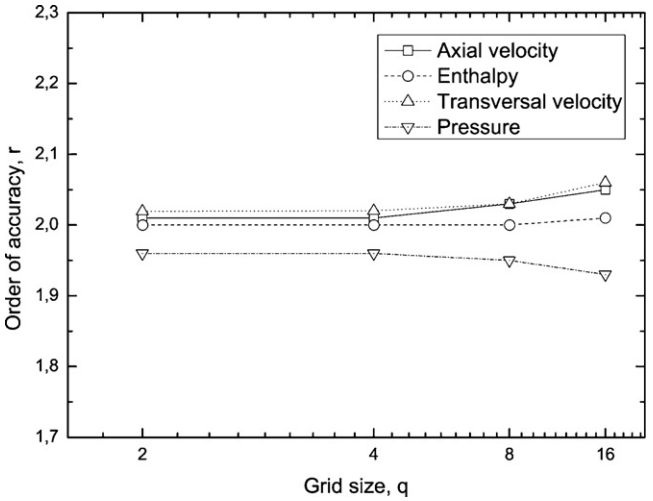

Fig. 15. Observed order of accuracy for axial and transversal velocities, enthalpy and pressure.

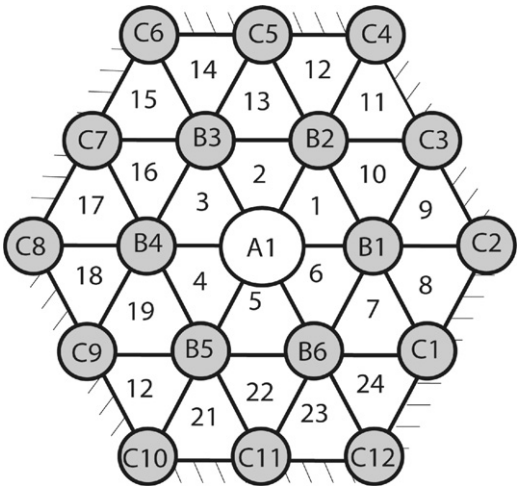

Fig. 16. Arrangement of 24 sub-channels.

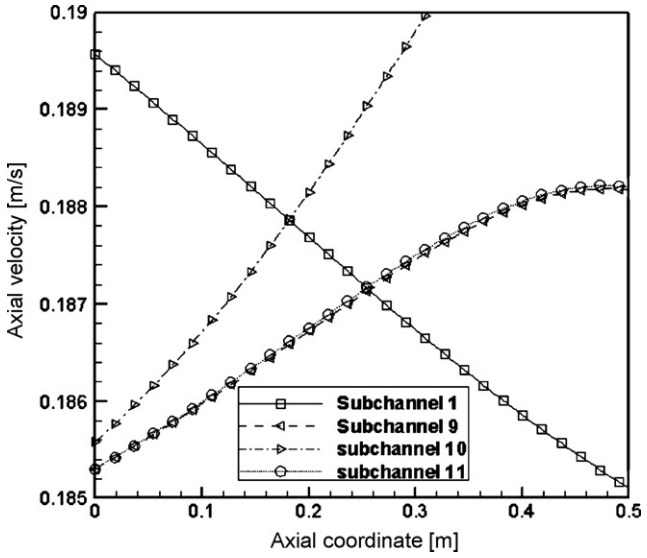

Fig. 17. Axial velocity profile for some sub-channels of the studied configuration.

the SIMPLE algorithm, the problem variables are iteratively updated over the considered sub-channel. In this level, it is inefficient to solve the governing equations accurately in the same sub-channel, since more inner iterations can cause the divergence of the outer loop sweeping the different sub-channels. On the other hand, few iteration in the inner loop during all iterative process provide easily the convergence of the outer loop but with erroneous results, because the simple algorithm must converge correctly to ensure the verification of the continuity equation. To solve this problem, we have used dynamical convergence criteria in the inner loop. At the beginning of the iterative procedure, this criterion requires little iteration. The number of iterations is increased dynamically during the iterative procedure.

4.4. Verification of SACATRI code simulating an array of sub-channels

The verification benchmarks proposed in the previous paragraph can be applied at the time of the code development. They consist of an analytical solution for simplified configurations described in the first and second test. If the previous verification tests give satisfactory results, it is important to submit the code to verification in more general configuration closer to reality, when the different equations of the model are solved for an array of sub-channels. In this context, the last step of SACATRI verification procedure consists to verify the code for an array of 24 sub-channels. Fig. 16 illustrates the sub-channel configuration employed for this verification test. The reactor inputs implemented into SACATRI code are provided in Table 6.

However, for the present case, manufacturing analytical solutions becomes a very complicated procedure, because it requires incorporating source terms, initial and boundary conditions for all sub-channels. As explained above, when the analytical solution does not exists, three different numerical solutions on three different resolution meshes are required in order to calculate the observed order of accuracy.

The observed order of accuracy and the relative discretization error are calculated for temperature, axial and transversal velocities by using Eqs. (17) and (22), respectively. The three meshes employed are $q_1 = 20$, $q_2 = 40$ and $q_3 = 80$ where the grid refinement factor $\bar{Q}$ is equal to 2.

Profiles of axial and transversal velocities, temperature and pressure for some sub-channels are presented in Figs. 17–20. Fig. 21 shows the observed order of accuracy r obtained. It is clear that SACATRI code reproduces perfectly the theoretical order of accuracy ($r = 2$).

In the asymptotic grid convergence region, the discretization error should drop as $1/\bar{Q}^r$. In the present case we have found that the calculated observed order of accuracy is equal to 2. Since the grid is refined by a factor of 2, then the relative discretization error for the three resolution meshes used, should obeys, in the asymptotic

Table 6
Data inputs implemented into SACATRI code.

Total number of fuel elements in the core	24
Fuel diameter (m)	0.0373
Control fuel diameter (m)	0.0340
Pitch (m)	0.043536
Unheated core length at inlet (m)	0.094
Unheated core length at outlet (m)	0.066
Fuel element heated length (m)	0.381
Coolant channel height (m)	0.541
Absolute pressure at the top of the core (Pa)	1.5
Coolant inlet temperature (°C)	33.1
Axial power peaking factor	1.3
Transversal hydraulic resistance ξ_{ik}	0.5

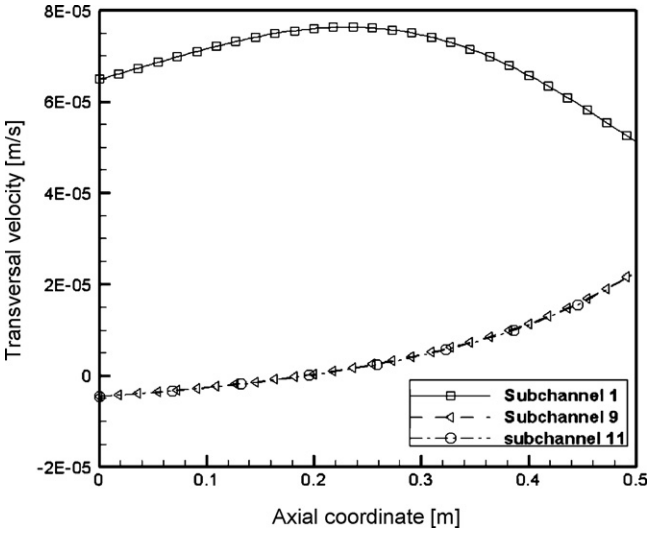

Fig. 18. Transversal velocity profile for some sub-channels of the studied configuration.

Table 7
The ratio of $RDE_{q\,(coarse\ mesh)}$ to $RDE_{q\,(fine\ mesh)}$ calculated for temperature (T), axial and transversal velocities (v and w).

Sub-channel number	Axial velocity (v)		Temperature (T)		Transversal velocity (w)	
	$\frac{RDE_{q_1 v}}{RDE_{q_2 v}}$	$\frac{RDE_{q_1 v}}{RDE_{q_3 v}}$	$\frac{RDE_{q_1 v}}{RDE_{q_2 v}}$	$\frac{RDE_{q_1 v}}{RDE_{q_3 v}}$	$\frac{RDE_{q_1 v}}{RDE_{q_2 v}}$	$\frac{RDE_{q_1 v}}{RDE_{q_3 v}}$
1	4.6	16.12	4.19	16.15	4.08	16.07
3	4.5	16.12	4.19	16.15	4.07	16.06
5	4.5	16.12	4.19	16.15	4.07	16.06
7	4.9	16.07	4.16	16.13	4.07	16.06
9	3.6	15.96	4.19	16.15	4.08	16.06
13	4.9	16.07	4.16	16.13	4.07	16.06
16	4.09	16.07	4.16	16.13	4.07	16.06
19	4.09	16.07	4.16	16.13	4.07	16.06
21	3.96	15.97	4.19	16.15	4.08	16.07
24	3.97	15.97	4.19	16.15	4.07	16.07

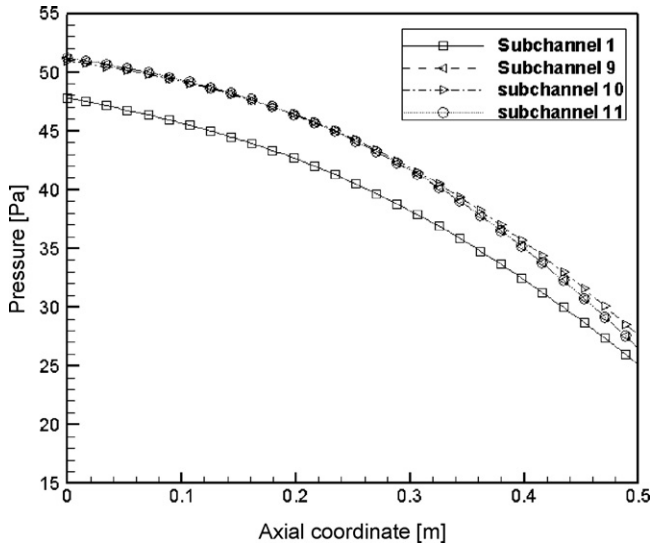

Fig. 19. Pressure profile for some sub-channels of the studied configuration.

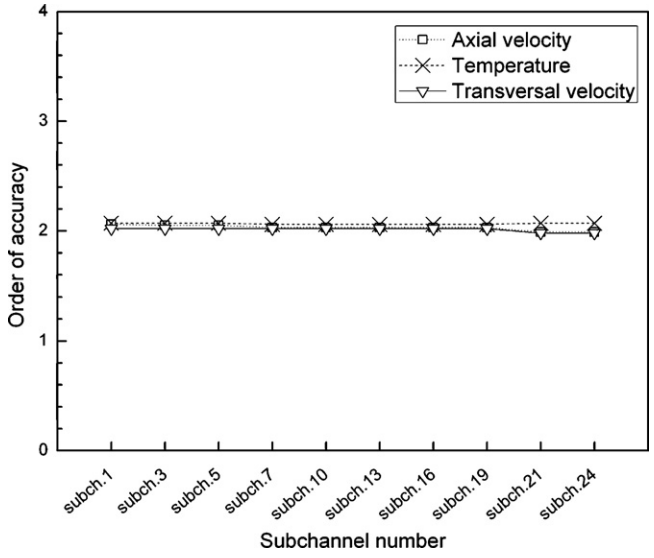

Fig. 21. Observed order of accuracy calculated for some sub-channels of the studied configuration.

grid region, to the relationship:

$$RDE_{q_{1\phi}} = 4 \times RDE_{q_{2\phi}} = 16 \times RDE_{q_{3\phi}}$$

The ratio of RDE_{φ} calculated for coarse mesh to RDE_{φ} calculated for fine mesh is summarized in Table 7. The obtained results are closed to the exact theoretical values 4 and 16 corresponding to $(RDE_{q_1 v}/RDE_{q_2 v})$ and $(RDE_{q_1 v}/RDE_{q_3 v})$, respectively.

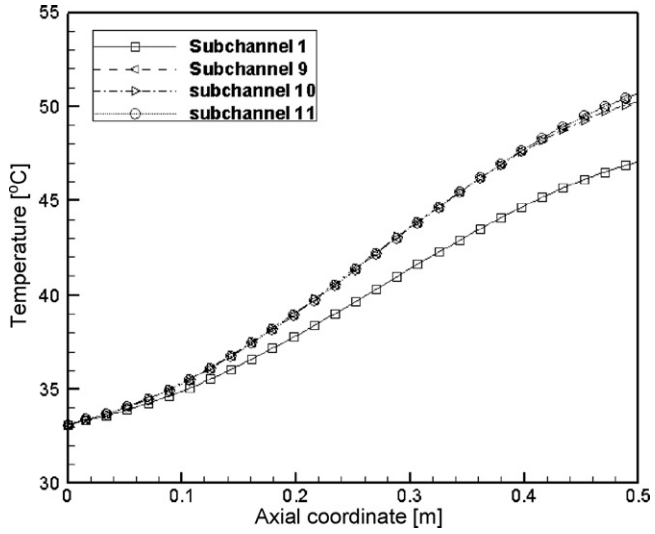

Fig. 20. Temperature profile for some sub-channels of the studied configuration.

5. Conclusion

Validation and verification (v&v) of any simulation code is critical since one cannot be confident that the numerical results are obtained with an acceptable degree of accuracy, unless it has been demonstrated that the code does what it should do. v&v activities help the code developers and users to confirm that a right simulation code is elaborated accurately, and allow improving the quality of the software. Verification is a purely mathematical exercise that examines the correctness of the solution to a given set of equations. Corroboration of the physics modeling accuracy of a computational simulation is the subject related to validation and is not the focus of this present work.

In this paper, emphasis is given on verification activities addressed to thermal-hydraulic problems. This work deals with code and solution verification of thermal-hydraulic codes based on the sub-channel approach. The verification activities proposed are applied in the verification of SACATRI code developed to simulate the thermal-hydraulic behaviour of the Moroccan TRIGA reactor. Code verification approach used in this study is based mainly on the combination of the method of manufactured solutions and the verification of the order of accuracy. For solution verification of SACATRI code, emphasis is given to estimate numerical errors

resulting from discretization of the governing thermal-hydraulic equations.

In this paper, we have detailed the different steps followed to construct exact analytical benchmarks for verifying SACATRI code. The application of the proposed benchmarks has been helpful during the development of the code, resulting in a rigorous process for finding pre-existing coding mistakes and bugs.

References

ANSYS, 2005. ANSYS CFX 10.0 Users Manual, ANSYS Inc., July 2005.

Austregesilo, A., Bals, C., Hora, A., Lerchl, G., Romstedt, P., 2003. ATHLET, Mod 2.0 Cycle A, Models and Methods, GRS-P-1, vol. 4, Gesellschaft für Anlagen- und Reaktorsicherheit (GRS) mbH, Germany.

AIAA, 1998. Guide for the Verification and Validation of Computational Fluid Dynamics Simulations. American Institute of Aeronautics and Astronautics, AIAA-G-077-1998.

Babuska, I., Oden, J.T., 2004. Verification and validation in computational engineering and science: basic concepts. Comput. Methods Appl. Mech. Eng. 193 (36–38), 4057–4066.

Botella, O., Peyret, R., 2001. Computing singular solutions of the Navier–Stokes equations with the Chebyshev-Collocation Method. Int. J. Numer. Methods Fluids 36 (2), 125–163.

Cheng, X., Schulenberg, T., Bittermann, D., Rau, P., 2003. Design analysis of core assemblies for supercritical pressure conditions. Nucl. Eng. Des. 223 (3), 279–294.

Christensen, M.J., Thayer, T.H., 2001. The Project Manager's Guide to Software Engineering's Best Practices. IEEE Computer Society, Los Alamos, CA.

FLUENT, 2005. FLUENT, version 6.2.16, 2005. FLUENT Inc., 10 Cavendish Court, Centerra Resource Park, Lebanon, NH 03766.

Han, K., Seo, K., Hwang, D., Chang, S.H., 2006. Development of a thermal hydraulic analysis code for gas-cooled reactors with annular fuels. Nucl. Eng. Des. 236 (2), 164–178.

International Atomic Energy Agency, 2005. Natural circulation in water cooled nuclear power plants, IAEA-TECDOC-1474.

Jiang, Y., Songtao, W., Baoshan, 2007. Development of sub-channel analysis code for CANDU-SCWR. Prog. Nucl. Energ. 49 (4), 334–350.

Knupp, P., Salari, K., 2002. Verification of Computer Codes in Computational Science and Engineering. Chapman & Hall/CRC, Boca Raton, FL.

Merroun, O., Almers, A., El Bardouni, T., 2008. Manufactured solution for verification of the 3D Thermalhydraulic SACATRI code. In: Proc. CHT-08 on Advances in Computational Heat Transfer, Begell House, New york, ISBN 978-1-56700-252-2.

Merroun, O., Almers, A., El Bardouni, T., 2007. Thermalhdraulic modeling and analysis of the hot channel of the Moroccan TRIGA MARK II research reactor. Proc. First Int. Conf on Physics and Technology of Reactors and Applications, Marrakech, Morocco, March 14–16, volume II, pp. 39.

Mele, I., 1993. TRISTAN, a computer program for calculating natural convection flow parameters in TRIGA Core. In: Regional Meeting, Nuclear Energy in Central Europe Present and Perspectives, Portorož, Slovenia, June 13–16.

Macdougall, J.D., Lillington, J.N., 1984. The SABRE code for fuel rod cluster thermo-hydraulics. Nucl. Eng. Des. 82 (2–3), 171–190.

Madeline, A.F., Miller, W.S., 1999. Three-dimensional coupled kinetics/thermal-hydraulic benchmark TRIGA experiments. Ann. Nucl. Ener. 27 (9), 771–790.

NUREG-5535, 2001. RELAP5/MOD3.3 code manual. User's guide and input requirements, vol. II. December 2001. U.S. Nuclear Regulatory Commission.

Oberkampf, W.L., Trucano, T.G., 2002. Verification and validation in computational fluid dynamics. Prog. Aerospace Sci. 38 (3), 209–272.

Oberkampf, W.L., Trucano, T.G., 2008. Verification and validation benchmarks. Nucl. Eng. Des. 238 (3), 716–743.

Oberkampf, W.L., Barone, M.F., 2004. Measures of Agreement Between Computation and Experiment: Validation Metrics. 34th AIAA Fluid Dynamics Conference. American Institute of Aeronautics and Astronautics, Portland, OR, AIAA Paper 2004-2626.

Patankar, S.V., 1980. Numerical Heat Transfer and Fluid Flow. Hemisphere, New York.

Roache, P.J., 2002. Code verification by the method of manufactured solutions. J. Fluid Eng. 124 (1), 4–10.

Roy, C.J., 2005. Review of code and solution verification procedures for computational simulation. J. Comput. Phys. 205 (1), 131–156.

Roache, P.J., 1998. Verification and Validation in Computational Science and Engineering. Hermosa Publishers, Albuquerque, NM.

Rowe, D.S., 1973. COBRA IIIC: a digital computer code for steady state and transient thermal-hydraulic analysis of rod bundle nuclear fuel elements. In: BNWL-1695. Battelle Pacific Northwest Laboratories, Richland, WA.

Smith, R.S., 1992. Comparison of NCTRIGA results to GA data, NCTRIGA input format and revision of NATCON, Intra-Laboratory Memo, Argon National Laboratory.

Shyy, W., Garbey, M., Appukuttan, A., Wu, J., 2002. Evaluation of Richardson extrapolation in computational fluid dynamics. Num. Heat. Trans. Part B 41 (2), 139–164.

Teschendorff, V., Austregesilo, H., Lerchl, G., 1996. Methodology, status and plans for development and assessment of the code ATHLET. In: Proceedings of the OECD/CSNI Workshop on Transient Thermal-hydraulic and Neutronic Codes Requirements Annapolis, USA, November 5–8, pp. 112–128.

Toumi, I., Bergeron, A., Gallo, D., Royer, E., Caruge, D., 2000. FLICA-4: a three-dimensional two-phase flow computer code with advanced numerical methods for nuclear applications. Nucl. Eng. Des. 200 (1–2), 139–155.

Veloso, M.A.F. 2004. Analise termofluidodinâmica de reactores nucleares de pesquisa refrigerados a agua em regime de convecção natural, M.Sc Thesis, Campinas, Faculdade de Engenheria Quimica, Brasil.

Wheeler, C.L., 1976. COBRA-IV-I: An Interim Version of COBRA Thermal-Hydraulic Analysis of Rod Bundle Nuclear Fuel Elements and Cores. Pacific Northwest Laboratories, USA.

William, T.S.H.A., 1980. An overview on rod-bundle thermal-hydraulic analysis. Nucl. Eng. Des. 62 (1–3), 1–24.

Yoo, Y.J., Hwang, D.H., Sohn, D.S., 1999. Development of a subchannel analysis code MATRA applicable to PWR and ALWRs. J. KNS 31, 314–327.